IEEE Access
Multidisciplinary | Rapid Review | Open Access Journal

Received 14 April 2023, accepted 1 May 2023, date of publication 25 May 2023, date of current version 1 June 2023.

Digital Object Identifier 10.1109/ACCESS.2023.3280054

RESEARCH ARTICLE

Analysis of Operating Characteristics of Variable Speed Pumped Storage Motor-Generator

HU JINMING[1,2], TAO DAJUN[1], SUN YUTIAN[2], ZHANG CHUNLI[2], LI GUIFEN[2], AND HU GANG[2]

[1]National and Local Joint Engineering Research Center of Large Electric Machines and Heat Transfer Technology, Harbin University of Science and Technology, Harbin 150080, China
[2]Harbin Institute of Large Electric Machinery, Harbin Electric Machinery Company Ltd., Harbin 150040, China

Corresponding author: Tao Dajun (tao.dj@163.com)

This work was supported in part by the National Natural Science Foundation of China under Grant 51407050 and Grant 51777048, and in part by the Natural Science Foundation of Heilongjiang Province under Grant TD2021E002.

ABSTRACT Large-scale variable-speed pumped storage motor-generator adopts rotor winding AC excitation technology, which can adapt to the regulation requirements of wide speed range and wide power variation. In order to adapt to the demand of dynamic change of multiple operating conditions of pumped storage motor-generator, combined with the characteristics of bi-directional energy flow of variable speed motor-generator, and considering the complex control strategy due to its two operating modes of power generation and electric power, it is the basis to realize the stable operation of the system to clarify the constraint law affecting the electrical quantity of motor-generator under different operating conditions. In this paper, the mathematical model of variable speed pumped storage motor is established by using the magnetic field positioning vector control technology, and the mathematical model of variable speed pumped storage motor is derived to analyze the operating characteristics of the motor. The model is used to calculate and analyze the electrical quantities during the speed regulation, active power regulation and reactive power regulation of the power motor, and to investigate the changes of electrical quantities such as stator and rotor current, rotor voltage, rotor active power, rotor reactive power and stator power angle during the change of working conditions. The accuracy of the mathematical model was verified by comparison using a 10MW prototype test. It is a necessary theoretical reference for the analysis of variable speed pumped storage motor-generator operating conditions.

INDEX TERMS Pumped storage power plant, variable speed generator motor, operating characteristics, prototype test.

I. INTRODUCTION

With the development of national clean energy strategy, one of the important ways to achieve clean power supply is by increasing the proportion of renewable energy sources such as wind and solar power to the grid [1], [2]. However, considering the intermittent and random characteristics of wind and solar power generation, smoothing out the asymmetric peak-to-valley difference between power and load is a basic requirement for stable grid operation, and pumped storage is one of the important ways to achieve large-scale peak shaving and valley filling and increase grid consumption of renewable energy power generation. 2014, the National Development and Reform Commission issued the ''Opinions on Promoting the Healthy and Orderly Development of Pumped Storage Power Plants Issues'' [3], [4]. Pumped storage units are usually of two types: constant-speed generating motors and variable-speed units. Compared with constant-speed generator motors, variable-speed generator motors have wider head adaptability and more efficient pump turbine operating characteristics [5], [6]. Most of the hydraulic resources in China are sediment rivers, and the water head varies greatly in different periods. Compared with conventional constant-speed synchronous pumped storage units, variable-speed pumped

The associate editor coordinating the review of this manuscript and approving it for publication was Amin Mahmoudi.

storage units can quickly respond to adjust the speed when the water head changes, so that the generator set always runs near the optimal speed of the turbine, which reduces the vibration, cavitation and wear of the hydro generator set, prolongs the life of the set, and improves the operating efficiency [7].

At present, China is in a blank state in the construction of variable speed pumped storage power plants, and there is an urgent need for localization. Scholars at home and abroad have done a lot of research work in the study of variable speed generator motor and have achieved rich research results. The literature [8] derived the mathematical expressions of motor operating parameters by analyzing the basic equations, equivalent circuit and space-time vector diagram of a doubly-fed generator, but the derived formulas are not easy to calculate and understand, and they are not considered from the decoupling perspective. In the literature [9], based on the principle of doubly-fed wind turbine, a static model of doubly-fed generator is established, which can calculate and analyze the parameters of generator resistance and reactance, and illustrate the design characteristics of doubly-fed asynchronous wind turbine. A 6.5 MW variable speed generator motor designed in the literature [10] provides some reference test data. The literature [11] describes the dynamic response characteristics of a 250 MW variable speed generator motor at Tehri power station in case of failure in electric mode. The literature [12] established a computational model for the hydraulic transition process of water-machine-electric coupling in pumped storage power plants using stator voltage directed vector control strategy, which has some reference value in decoupling control. In the literature [13], the Nyquist array theory in multivariate frequency domain analysis theory was used to analyze and control the stability of small disturbances in doubly-fed wind power grid-connected systems. In the paper [14], an accurate electromagnetic transient simulation model for fast start-up of an actual doubly-fed wind turbine in a wind farm in Mengxi, China, under full operating conditions was established. In the paper [15], a method was proposed to analyze the stator-side reactive power characteristics and regulation mechanism of the turbine based on the V-shaped curve. In the literature [16], the impedance characteristics of doubly-fed induction generators were studied for different wind speeds and different powers. In the paper [17], a transient simulation model of doubly-fed wind turbine was established and the feasibility of the control strategy was verified by simulation. In the literature [18], a program for online identification of stator and rotor inductance based on stator current and voltage sensors was developed. In the literature [19], a sequential impedance model of the doubly-fed induction generator system was developed based on the complex transfer function. In the literature [20], based on the basic operating equations of wind turbines, an expression for the maximum regulated power during rotor over-speed of doubly-fed wind turbines was derived, pointing out that the bi-directional adjustable frequency power of wind turbines is constrained by the power reservation factor and the maximum regulated power. In the literature [21], based on the load optimization theory, a method to find the minimum unit flow on the equal unit power curve was proposed for improving the optimal speed finding strategy.

Analyzing the above literature, we can find that they all focus on the research of control strategy, and the research and understanding of the operating characteristics of variable speed motor-generator are still in the initial stage. In this paper, considering the special characteristics of variable-speed pumped storage units and the complexity of their operating conditions, the analytical calculation and experimental verification of the change law of electrical quantities during the change of different operating conditions of the generator motor are carried out, which provides technical support and reference for the design and manufacture of the unit and its safe and stable operation.

II. DERIVATION OF MATHEMATICAL MODELS FOR OPERATIONAL CHARACTERIZATION

According to the motor convention, the stator magnetic field is positioned to the d-axis in the vector control system as a way to achieve relative standstill by placing the rotating sympathetic variable in a synchronously rotating coordinate system. The voltage equation, magnetic chain equation, motion equation and power equation of the variable speed generator motor in the synchronous rotating dq-axis coordinate system are expressed in Eqs. (1)-(4).

The voltage equation is as follows.

$$\begin{cases} u_{ds} = R_s i_{ds} + \dfrac{d\psi_{ds}}{dt} - \omega_s \psi_{qs} \\ u_{qs} = R_s i_{qs} + \dfrac{d\psi_{qs}}{dt} + \omega_s \psi_{ds} \\ u_{dr} = R_r i_{dr} + \dfrac{d\psi_{dr}}{dt} - \omega_r \psi_{qr} \\ u_{qr} = R_r i_{qr} + \dfrac{d\psi_{qr}}{dt} + \omega_r \psi_{dr} \end{cases} \tag{1}$$

The equation of the magnetic chain is as follows.

$$\begin{cases} \psi_{ds} = L_s i_{ds} + L_m i_{dr} \\ \psi_{qs} = L_s i_{qs} + L_m i_{qr} \\ \psi_{dr} = L_m i_{ds} + L_r i_{dr} \\ \psi_{qr} = L_m i_{qs} + L_r i_{qr} \end{cases} \tag{2}$$

The equations of motion are as follows.

$$\begin{cases} T_{em} = \dfrac{3}{2} p(\psi_{ds} i_{qs} - \psi_{qs} i_{ds}) \\ T_{em} - T_m = J \dfrac{d\Omega_m}{dt} + D\Omega_m \end{cases} \tag{3}$$

The power equation is as follows.

$$\begin{cases} P_s = \dfrac{3}{2}(u_{ds} i_{ds} + u_{qs} i_{qs}) \\ P_r = \dfrac{3}{2}(u_{dr} i_{dr} + u_{qr} i_{qr}) \\ Q_s = \dfrac{3}{2}(u_{qs} i_{ds} - u_{ds} i_{qs}) \\ Q_r = \dfrac{3}{2}(u_{qr} i_{dr} - u_{dr} i_{qr}) \end{cases} \tag{4}$$

where the quantity with d in the lower corner is the d-axis quantity and the quantity with q in the lower corner is the q-axis quantity. u_s, u_r are the stator and rotor voltages respectively. i_s, i_r are the stator and rotor currents respectively. R_s, R_r are the stator and rotor resistances respectively. L_s, L_r, L_m are the stator and rotor inductances and excitation inductances respectively. ω_s, ω_r are the stator and rotor angular frequencies respectively. Ω_m is the mechanical angular velocity. p is the pole pair. ψ_s, ψ_r are stator and rotor magnetic chains. T_{em}, T_m are electromagnetic torque and mechanical torque. J, D are rotational inertia and friction coefficient. P_s, P_r are stator active power and rotor active power respectively. Q_s, Q_r are stator reactive power and rotor reactive power respectively.

Since the magnetic field is localized to the d-axis, the magnetic chain satisfies the following equation.

$$\begin{cases} \psi_{ds} = \psi_s \\ \psi_{qs} = 0 \end{cases} \tag{5}$$

Substituting equation (5) into equation (2), it can be deduced that.

$$\begin{cases} i_{ds} = \dfrac{\psi_s - L_m i_{dr}}{L_s} \\ i_{qs} = -\dfrac{L_m i_{qr}}{L_s} \end{cases} \tag{6}$$

Substituting equation (6) into equations (3) and (4), it can be deduced that.

$$\begin{cases} T_{em} = -\dfrac{3}{2} p \psi_{ds} \dfrac{L_m}{L_s} i_{qr} \\ P_s = -\dfrac{3}{2} u_s \dfrac{L_m}{L_s} i_{qr} \\ Q_s = \dfrac{3}{2} u_s \left(\dfrac{\psi_s}{L_s} - \dfrac{L_m}{L_s} i_{dr} \right) \end{cases} \tag{7}$$

From equation (7), it can be seen that the electromagnetic torque decoupling is controlled by i_{qr}, the stator active power decoupling is controlled by i_{qr}, and the stator reactive power decoupling is controlled by i_{dr}. Further derivation and collation of the previous equations can establish the mathematical model of operating characteristics analysis of variable speed generator motor, whose constraints are speed n, stator active power P_s or electromagnetic torque T_{em} and stator reactive power Q_s, which are the external variables of the operation of variable speed generator motor and change accordingly during the change of working conditions Under the steady state operation of the motor, bringing equation (5) into equation (1) can be obtained as follows.

$$\begin{cases} u_{ds} = R_s i_{ds} \\ u_{qs} = R_s i_{qs} + \omega_s \psi_s \end{cases} \tag{8}$$

From equations (6) and (7), it can be deduced that.

$$\begin{cases} i_{ds} = \dfrac{2}{3} \dfrac{Q_s}{\omega_s \psi_s} \\ i_{qs} = \dfrac{2}{3} \dfrac{T_{em}}{p \psi_s} \end{cases} \tag{9}$$

Substituting equations (8) and (9) into equation, the following relationship is derived for the unknown quantity ψ_s with respect to the known quantities ω_s, T_{em}, Q_s, u_s, R_s and p.

$$\omega_s^2 (\psi_s)^4 + \left(R_s \frac{4}{3} \frac{T_{em} \omega_s}{p} - u_s^2 \right) (\psi_s)^2 + \left(R_s \frac{2}{3} \right)^2 \left(\left(\frac{Q_s}{\omega_s} \right)^2 + \left(\frac{T_{em}}{p} \right)^2 \right) = 0 \tag{10}$$

Eqs. (10) is a quadratic equation with the following solutions.

$$\psi_s = \sqrt{\frac{-B \pm \sqrt{B^2 - 4AC}}{2A}} \tag{11}$$

where.

$$\begin{cases} A = \omega_s^2 \\ B = R_s \dfrac{4}{3} \dfrac{T_{em} \omega_s}{p} - u_s^2 \\ C = \left(R_s \dfrac{2}{3} \right)^2 \left(\left(\dfrac{Q_s}{\omega_s} \right)^2 + \left(\dfrac{T_{em}}{p} \right)^2 \right) \end{cases}$$

The stator voltage is known from equation (8) as follows.

$$\begin{cases} u_{ds} = R_s i_{ds} \\ u_{qs} = R_s i_{qs} + \omega_s \psi_s \\ \theta_{us} = \angle (u_{ds}, u_{qs}) \end{cases} \tag{12}$$

The stator current is known from equation (9) as follows.

$$\begin{cases} i_{ds} = \dfrac{Q_s}{\frac{3}{2} \omega_s \psi_s} \\ i_{qs} = \dfrac{T_{em}}{\frac{3}{2} p \psi_s} \\ i_s = \sqrt{(i_{ds}^2 + i_{qs}^2)} \\ \theta_{is} = \angle (i_{ds}, i_{qs}) \end{cases} \tag{13}$$

Transformation of equation (6) results in the following equation for the rotor current.

$$\begin{cases} i_{dr} = \dfrac{\psi_s - L_s i_{ds}}{L_m} \\ i_{qr} = -\dfrac{L_s}{L_m} i_{qs} \\ i_r = \sqrt{(i_{dr}^2 + i_{qr}^2)} \\ \theta_{ir} = \angle (i_{dr}, i_{qr}) \end{cases} \tag{14}$$

Substitute equation (6) into (2) to find ψ_{qr}, and then substitute it into equation (1) to derive the rotor voltage as follows.

$$\begin{cases} u_{dr} = R_r i_{dr} - \omega_r \psi_{qr} = R_r i_{dr} - \omega_r \sigma L_r i_{qr} \\ u_{qr} = R_r i_{qr} + \omega_r \psi_{dr} = R_r i_{qr} + \omega_r \sigma L_r i_{dr} + \omega_r \dfrac{L_m}{L_s} \psi_s \\ u_r = \sqrt{(u_{dr}^2 + u_{qr}^2)} \\ \theta_{ur} = \angle (u_{dr}, u_{qr}) \end{cases} \tag{15}$$

The leakage inductance coefficient in the formula is as follows.

$$\sigma = \left(1 - \frac{L_m^2}{L_s L_r}\right)$$

From equation (2), the rotor magnetic chain is as follows.

$$\begin{cases} \psi_{dr} = L_m i_{ds} + L_r i_{dr} \\ \psi_{qr} = L_m i_{qs} + L_r i_{qr} \\ \psi_r = \sqrt{(\psi_{dr}^2 + \psi_{qr}^2)} \\ \theta_{\psi r} = \angle(\psi_{dr}, \psi_{qr}) \end{cases} \tag{16}$$

From equation (4), the stator and rotor active power and the stator and rotor reactive power are shown in the following equation.

$$\begin{cases} P_s = \frac{3}{2}(u_{ds} i_{ds} + u_{qs} i_{qs}) \\ P_r = \frac{3}{2}(u_{dr} i_{dr} + u_{qr} i_{qr}) \\ Q_s = \frac{3}{2}(u_{qs} i_{ds} - u_{ds} i_{qs}) \\ Q_r = \frac{3}{2}(u_{qr} i_{dr} - u_{dr} i_{qr}) \end{cases} \tag{17}$$

Since the excitation electromotive force E is 90° ahead of the stator magnetic chain, the angle of the excitation electromotive force is constant at 90° in the dq-axis coordinate system. The stator work angle can be obtained as follows.

$$\delta = 90° - \theta_{us} \tag{18}$$

After the derivation of the above model, a mathematical model for the analysis of the operating characteristics of a variable speed motor-generator consisting of equations (10) - (18) has been established. Using this model, electrical quantities such as stator and rotor currents, rotor voltages, rotor active power, rotor reactive power and stator power angle can be calculated for the speed regulation, active power regulation and reactive power regulation of the power motor. To facilitate the understanding of this operating characteristic analysis mathematical model, a block diagram of this mathematical model is given below, as shown in Fig. 1.

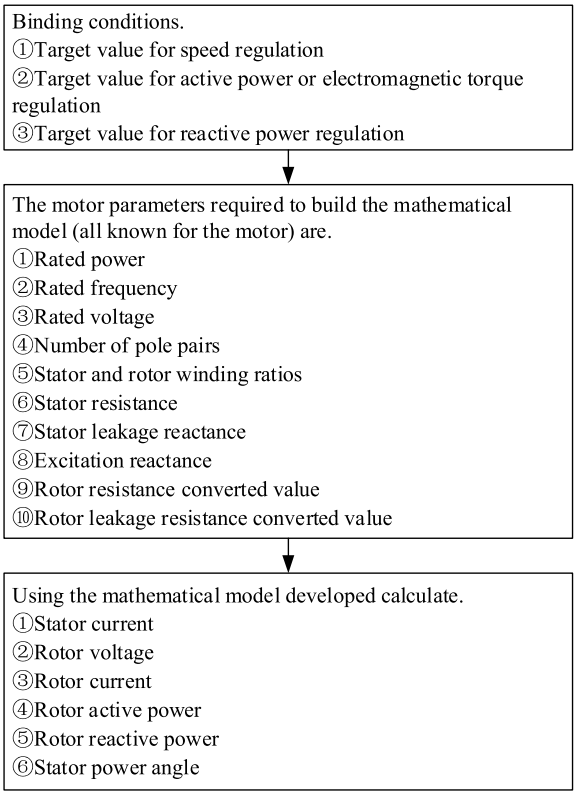

FIGURE 1. Block diagram of a mathematical model for the analysis of the operating characteristics of a variable speed motor-generator.

III. OPERATING CHARACTERISTICS ANALYSIS

This paper analyzes and calculates the operating characteristics of a 10MW variable speed motor prototype, including speed regulation under power generation condition, active power regulation under power generation to electric condition, and reactive power regulation under no-load condition, in order to investigate the changes of electrical quantities such as stator and rotor current, rotor voltage, rotor active power, rotor reactive power, and stator power angle during the condition change. The electrical quantities such as rotor current, rotor voltage, rotor active power, rotor reactive power, and stator power angle change during the change of operating conditions. The main parameters of the prototype are shown in Table 1.

TABLE 1. Main parameters of variable speed generator motor.

Rated parameters	Power generation mode	Electric mode	unit
Rated power	10	10.56	MW
Rated voltage	10.5	10.5	kV
Power Factor	0.9	0.98	-
Synchronous speed	500	500	r/min
Slip	±8	±8	%
Stator-rotor ratio	0.54	0.54	-
Stator resistance	0.0462	0.0462	Ω
Stator leakage resistance	0.969	0.969	Ω
Rotor resistance conversion value	0.0261	0.0261	Ω
Rotor leakage resistance discounted value	1.8701	1.8701	Ω
Excitation reactance saturation value	8.953	8.953	Ω

A. THE CHANGE LAW OF ELECTRICAL QUANTITY WHEN ADJUSTING THE SPEED UNDER THE POWER GENERATION CONDITION

In order to investigate the changes of electrical quantities such as stator and rotor currents, rotor voltage, rotor active power, rotor reactive power and stator power angle during speed regulation of variable speed generating motors, this paper uses the mathematical model established for operating

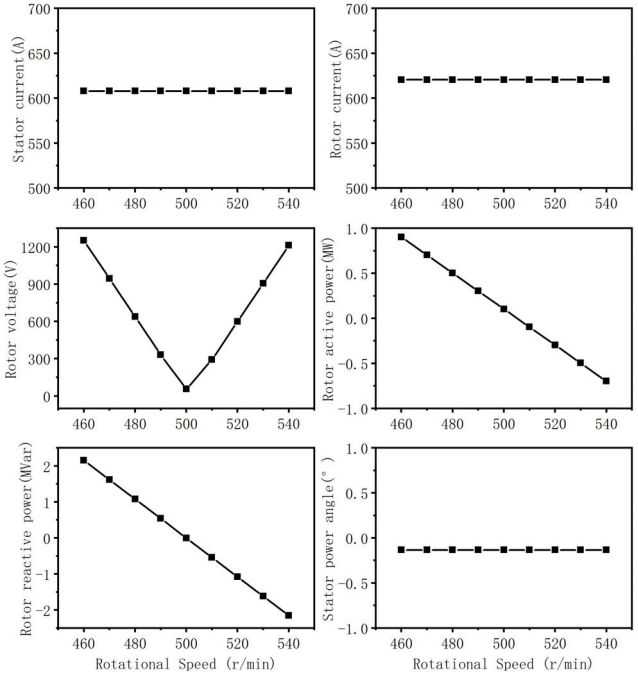

FIGURE 2. Curve of amplitude and power angle change of electrical quantity during speed regulation of power generation condition.

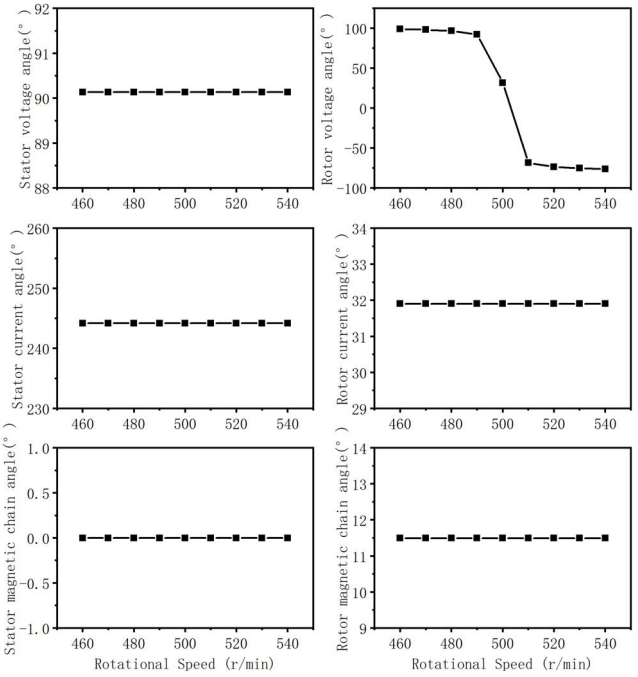

FIGURE 3. Angular change curve of electrical quantity during speed adjustment of power generation condition.

characteristics analysis to analyze the changes of electrical quantities during speed regulation under rated generating conditions of the prototype, the given constraints are: (i) speed regulation from 460-540 r/min, calculated at 10 r/min intervals; (ii) active power constant at 10 MW; and (iii) reactive power constant at 4.84 MVar. the variation of the relevant electrical quantities is shown in Figure 2.

From Fig. 2, it can be seen that the stator-side active and reactive power are constant, and the stator and rotor currents are constant when the speed is adjusted from 460-540 r/min, the rotor voltage shows a V-shape and is the smallest near the synchronous speed, the rotor active power is positive at the sub-synchronous speed, representing the absorption of active power from the net, and negative at the hyper-synchronous speed, representing the emission of active power to the net, the rotor reactive power is positive at the sub-synchronous speed, representing the absorption of reactive power from the net, and negative at the hyper-synchronous speed, representing the emission of reactive power to the net, the stator work angle is constant and small, and the motor is statically stable.

Since the phase diagram can visually observe the regulation of the electrical quantities when the working condition is transformed, this paper analyzes the angular change of the electrical quantities when the speed is regulated under the rated power generation condition of the prototype, defining the stator magnetic chain as 0°, as shown in Fig. 3. Based on this, the phase diagram of the prototype at sub-synchronous and hyper-synchronous speed is drawn as shown in Fig. 4.

From Fig. 3 and Fig. 4, it can be seen that the stator-side active and reactive power are constant, and the stator

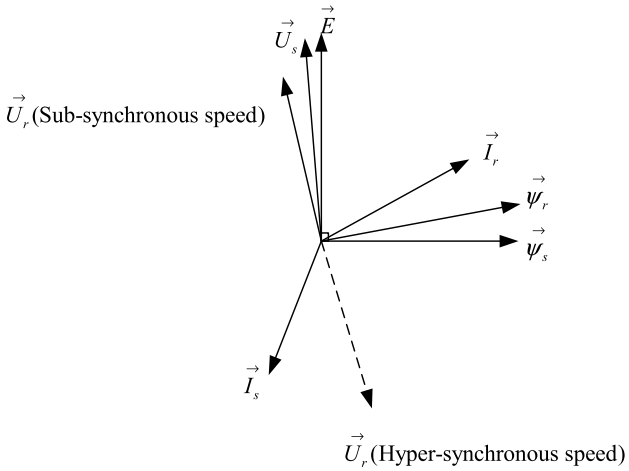

FIGURE 4. Phase diagram during power generation speed regulation.

voltage angle, stator-rotor current angle and stator-rotor magnetic chain angle are constant when the speed is adjusted from 460-540 r/min, the rotor voltage angle changes with the speed.

B. THE CHANGE LAW OF ELECTRICAL QUANTITY WHEN REGULATING THE ACTIVE POWER UNDER THE CONVERSION FROM POWER GENERATION TO ELECTRIC OPERATION

In order to investigate the changes of electrical quantities such as stator and rotor currents, rotor voltage, rotor active power, rotor reactive power and stator power angle during stator active regulation, this paper uses the mathematical

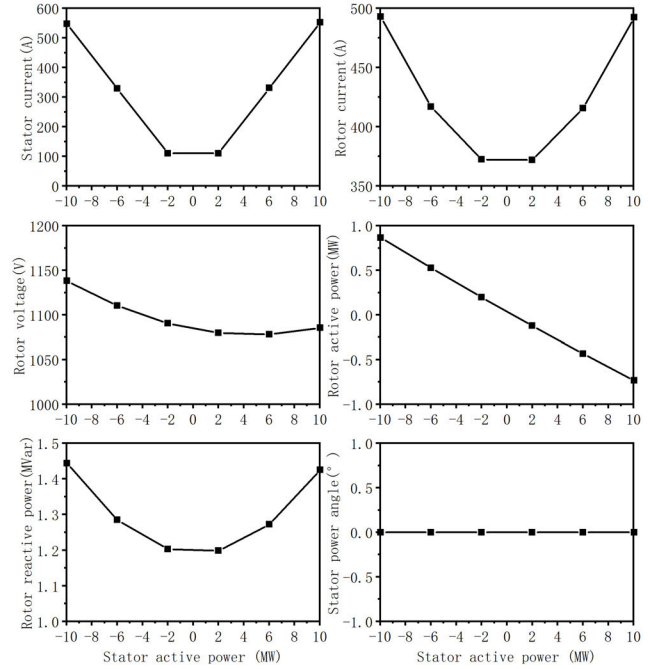

FIGURE 5. Amplitude and power angle change curve of electrical quantity during active regulation.

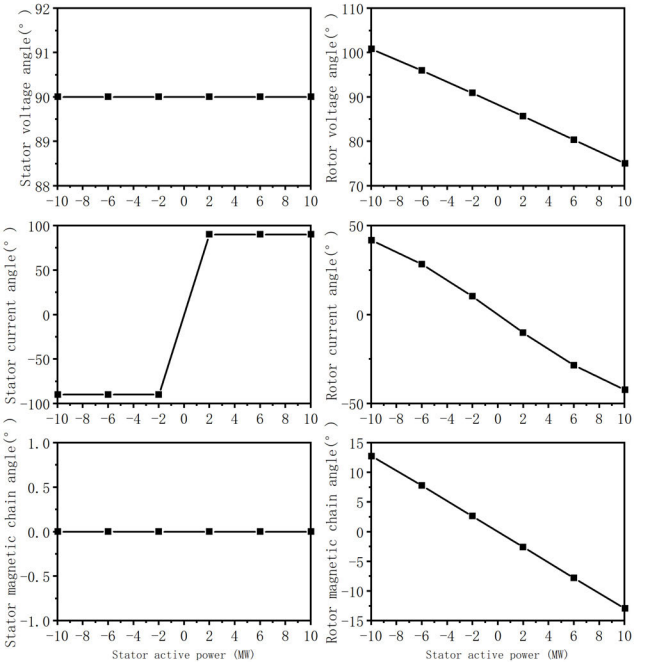

FIGURE 6. Angular change curve of electrical quantity during active regulation.

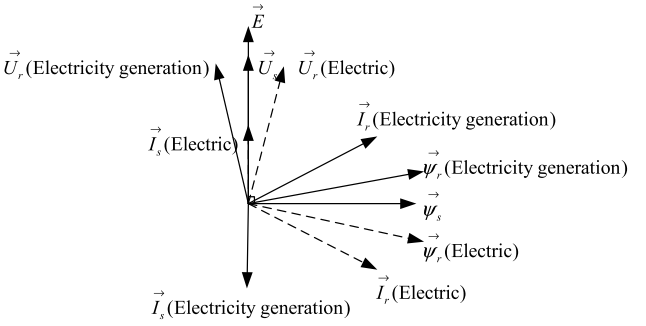

FIGURE 7. Phase diagram during active regulation.

model established for the analysis of operating characteristics to analyze the change of active power when regulating the prototype under the transition from generation to electric operation, the given constraints are: (i) speed at sub-synchronous 460r/min; (ii) active power regulation at 6 points for generation 10MW, generation 6MW, generation 2MW, electric 2MW, electric 6MW and electric 10MW respectively; and (iii) reactive power constant at 0MVar. the variation of the relevant electrical quantities is shown in Figure 5.

As can be seen from Figure 5, under the sub-synchronous 460r/min, stator reactive power is 0Var, when regulating active power under the conversion of power generation condition to electric condition, the stator-rotor current and rotor reactive power show V-shaped, rotor voltage is lower in electric condition, rotor active power gradually decreases and changes from absorbing active power to emitting active power, the stator work angle is constant 0.

The angular variation of the relevant electrical quantities was analyzed for the prototype when regulating the active power under the conversion from generation to electric operation at sub-synchronous 460r/min and stator reactive power of 0Var as shown in Fig. 6. Based on this, the phase diagram of the prototype is drawn as shown in Fig. 7.

From Fig. 6 and Fig. 7, it can be seen that the stator speed is constant, the stator reactive power is 0, and the stator voltage angle is constant at 90° when regulating the active power under the conversion from power generation to electric operation, the stator current angle is -90° in power generation and 90° in electric operation, the rotor voltage lags behind the excited electric potential in power generation and exceeds the excited electric potential in electric operation, the rotor current and rotor magnetic chain lag behind the stator magnetic chain in power generation and exceed the stator magnetic chain in electric operation.

C. THE CHANGE LAW OF ELECTRICAL QUANTITY WHEN REGULATING REACTIVE POWER IN NO-LOAD CONDITION

In order to investigate the changes of electrical quantities such as stator and rotor currents, rotor voltage, rotor active power, rotor reactive power and stator power angle during stator reactive power regulation of variable speed generating motors, this paper uses the mathematical model established for operating characteristics analysis to analyze the reactive power regulation of the prototype, the given constraints are: (i) rotational speed at sub-synchronous 460r/min; (ii) active power is constant at 0MW; (iii) reactive power regulation is issued at 11.11MVar, issued at 6.67MVar, issued at 2.22MVar, absorbed at 2.22MVar, absorbed at 6.67MVar, absorbed at

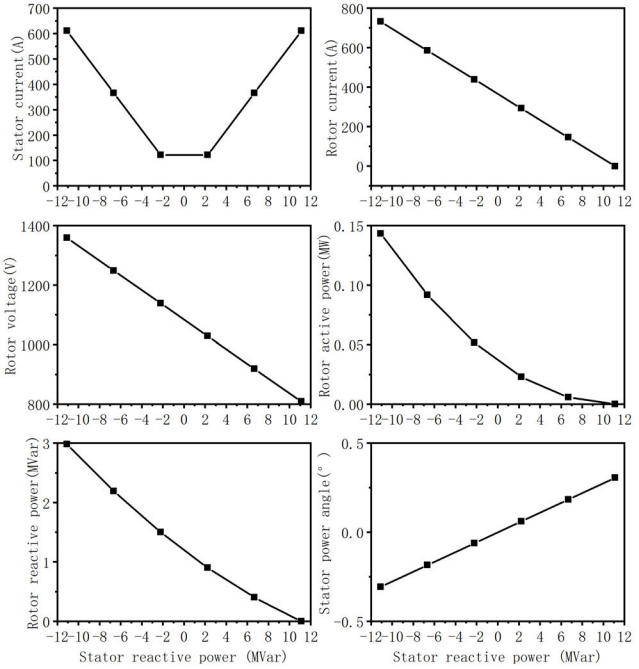

FIGURE 8. Amplitude and power angle change curve of electrical quantity during no-load condition reactive power regulation.

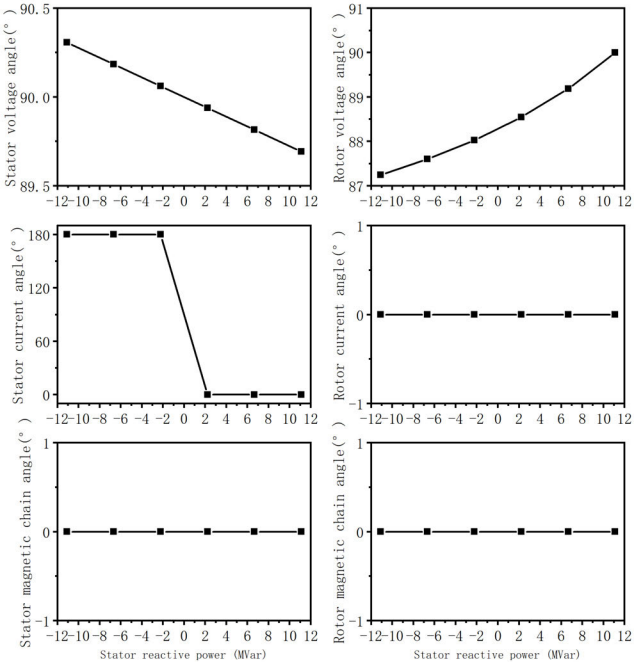

FIGURE 9. Angle change curve of electrical quantity during no-load condition reactive power regulation.

11.11MVar for a total of 6 points, in order to explore the static stability limit of the motor The maximum point of reactive power regulation is set as 11.11 MVar. the change of relevant electrical quantities is shown in Figure 8.

From Figure 8, we can see that under the sub-synchronous 460r/min, stator active power is 0W, stator reactive power from issuing reactive power to absorbing reactive power and gradually deep into phase, stator current decreases and then increases, rotor current, rotor voltage, rotor active power and rotor reactive power gradually decreases, stator work angle gradually increases, but in deep into phase, stator work angle is much less than 90°, which meets the static stability requirements, so it can be variable speed The generator motor can run in deep phase.

The angle change of the relevant electrical quantity is shown in Fig. 9 when the stator reactive power changes from issuing reactive power to absorbing reactive power and gradually entering the phase in depth under the sub-synchronous 460r/min and stator active power of 0W of the prototype is analyzed. Based on this, the phase diagram of the prototype when issuing reactive power and absorbing reactive power is drawn as shown in Fig. 10.

From Fig.9 and Fig.10, we can see that the stator speed is constant, stator active power is 0, stator reactive power from issuing reactive power to absorbing reactive power and gradually deep into the phase, the stator-rotor magnetic chain angle, rotor current angle is constant 0, rotor voltage angle gradually increases, stator work angle gradually increases and changes from negative to positive, and stator work angle only changes when adjusting stator reactive power.

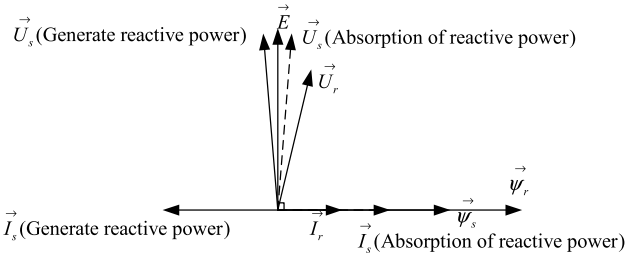

FIGURE 10. Phase diagram of reactive power regulation at no-load condition.

In summary, the mathematical model established for the analysis of operating characteristics was used to investigate the changes of electrical quantities such as stator and rotor currents, rotor voltage, rotor active power, rotor reactive power, and stator power angle during the change of three typical operating conditions: regulation of rotational speed under power generation, regulation of active power under conversion from power generation to electric operation, and regulation of reactive power under no-load operation, and the following conclusions were drawn:

(i) When adjusting the speed, the stator and rotor currents are constant; the rotor voltage is V-shaped and the smallest near the synchronous speed; the rotor active power is absorbed at the sub-synchronous speed and issued at the super-synchronous speed; the rotor reactive power is absorbed at the sub-synchronous speed and issued at the super-synchronous speed; the stator work angle is constant and small, the motor is statically stable; the stator voltage angle, the stator-rotor current angle and the stator-rotor

FIGURE 11. Variable speed motor-generator prototype test system.

magnetic chain angle are constant; the rotor voltage angle changes with the speed;

(ii) When regulating active power, the stator and rotor currents and rotor reactive power show a V-shape; rotor voltage is lower in electric service; rotor active power gradually decreases and changes from absorbing active power to emitting active power; stator power angle is constant at 0; stator voltage angle is constant at 90°; stator current angle is -90° when generating and 90° when electric; rotor voltage lags behind the excited electric potential when generating and overtakes it when electric; rotor current and rotor magnetic chain lags behind the stator magnetic chain when generating and overtakes it when electric;

(iii) When adjusting the reactive power, the stator current decreases and then increases; rotor current, rotor voltage, rotor active power and rotor reactive power gradually decrease; stator work angle gradually increases, but in deep phase, the stator work angle is much less than 90°, which meets the static stability requirements, so the variable speed power motor can run in deep phase; rotor magnetic chain angle and rotor current angle are constant 0; rotor voltage angle gradually increases; stator work angle gradually increases and The stator power angle only changes when the stator reactive power is adjusted.

IV. TEST VERIFICATION OF 10MW VARIABLE SPEED MOTOR-GENERATOR PROTOTYPE

In order to verify the accuracy of the calculation results of the mathematical model for variable speed motor-generator operation characteristics analysis, a 10MW variable speed pumped storage motor-generator prototype was fabricated and tested, including no-load test, speed regulation test, active power regulation test and reactive power regulation test. Fig.11 shows the test system diagram of the 10MW variable speed pumped storage generator prototype, which includes the tractor, gearbox, variable speed generator motor, excitation transformer, back-to-back converter, etc.

The test was carried out in accordance with GB/T 1029-2005 "Test Methods for Three-phase Synchronous Motors". The test conditions were limited by the capacity of the towing motor and the capacity of the local grid, so four tests were carried out: no-load characteristic test, no-load speed test, regulated active power test and regulated reactive power test. From the results of the analytical calculations using the mathematical model for operating characteristics analysis and the results of the test comparison, the universality and accuracy of the mathematical model established were well verified.

A. NO-LOAD CHARACTERISTIC TEST ANALYSIS

The no-load characteristics of the motor were tested in accordance with the standard, with the motor under test running off-grid and at 480r/min, the excitation current was adjusted and the stator terminal voltage recorded. The test data is shown in Table 2.

TABLE 2. No-load characteristics test results.

No.	Excitation current/A	Stator voltage/kV	Excitation reactance/Ω
1	44.10	2.25	15.93
2	65.27	3.29	15.74
3	85.07	4.27	15.68
4	105.17	5.23	15.53
5	125.10	6.14	15.33
6	145.30	6.95	14.94
7	189.33	8.26	13.62
8	219.13	8.88	12.66
9	254.30	9.43	11.58
10	299.30	9.95	10.38
11	349.07	10.40	9.30
12	388.93	10.70	8.59
13	399.00	10.76	8.42

For variable speed motor-generator, the core saturation is mainly reflected in the variation of excitation reactance, so the variation curve of excitation reactance with excitation current in no-load characteristic is plotted as shown in Fig.12.

From Fig. 12, it can be found that the excitation reactance of the variable speed motor-generator decreases gradually with the increase of excitation current, and it decreases faster in the saturation zone.

The excitation reactance curve is added to the mathematical model of operating characteristic analysis as a variable to calculate the no-load characteristic, and the result is shown in Fig. 13, and the analyzed value is basically consistent with the test value.

Since the excitation reactance in the motor parameters varies with the motor operating point, this step of the test work verifies on the one hand the accuracy of the calculation results of the mathematical model developed for the analysis of the operating characteristics at this operating condition, and on the other hand the influence of the changes in the excitation reactance parameter is taken into account in the subsequent comparison of the test conditions, improving the accuracy of the calculation.

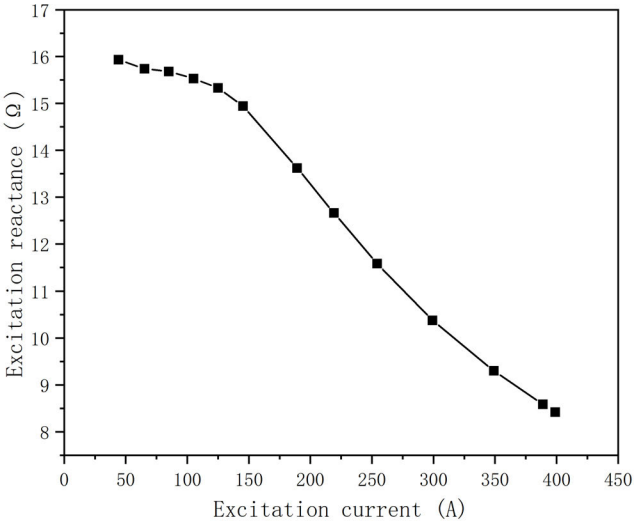

FIGURE 12. Excitation reactance variation curve with excitation current.

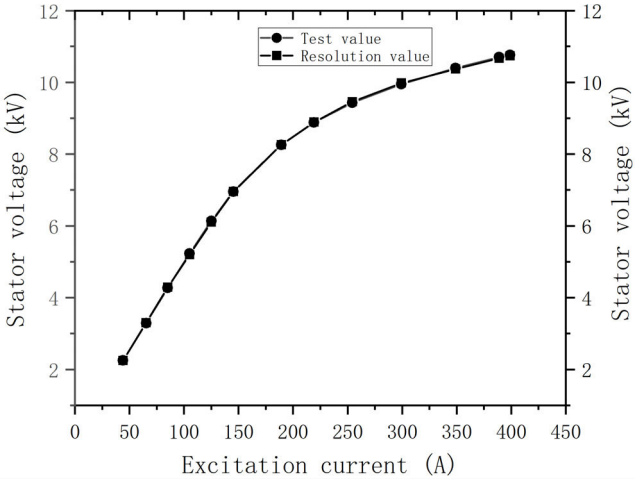

FIGURE 13. No-load characteristic comparison curve.

B. NO-LOAD SPEED REGULATION TEST ANALYSIS

In accordance with the standard motor no-load speed test, the stator side of the tested motor is running on the network, and the speed is adjusted within the range of the differential speed. Since the rotor side of the variable-speed motor is low-frequency excitation, the excitation voltage cannot be accurately tested using a voltage transformer, so the active power, reactive power, stator voltage, stator current and excitation current on the stator side are recorded, and the subsequent tests are the same, and the same working conditions are analyzed and calculated using the operating characteristic analysis model, and the comparison results data are shown in Table 3.The curves of stator and rotor currents versus speed at eight operating points during the no-load speed regulation test are plotted as shown in Fig.14.The stator active and reactive power symbols in the table are negative for emitted and positive for absorbed.

An inspection of the data in Table 3 and the comparison curves in Fig.14 shows that:

TABLE 3. Comparison of the results of the speed adjustment test.

Binding conditions	Stator current/A			Rotor current/A		
	Test value	Parse value	Err/ %	Test value	Parse value	Err/ %
point 1: ①n=460r/min ②Ps=253kW ③Qs=-204kVar	18.7	18.3	-2.4	335.8	341.6	1.7
point 2: ①n=470r/min ②Ps=311kW ③Qs=-195kVar	20.2	20.7	2.2	334.7	341.6	2.0
point 3: ①n=480r/min ②Ps=317kW ③Qs=-160kVar	19.8	20.0	1.0	336.2	340.4	1.2
point 4: ①n=490r/min ②Ps=281kW ③Qs=-177kVar	18.8	18.7	-0.7	335.5	341.0	1.6
point 5: ①n=510r/min ②Ps=296kW ③Qs=-188kVar	19.2	19.8	2.6	335.8	341.4	1.6
point 6: ①n=520r/min ②Ps=258kW ③Qs=-114kVar	16.2	15.9	-2.1	335.8	338.9	0.9
point 7: ①n=530r/min ②Ps=282kW ③Qs=-117kVar	24.7	24.9	0.8	335.3	339.0	1.1
point 8: ①n=540r/min ②Ps=306kW ③Qs=-109kVar	18.9	18.3	-3.3	335.3	338.7	1.0

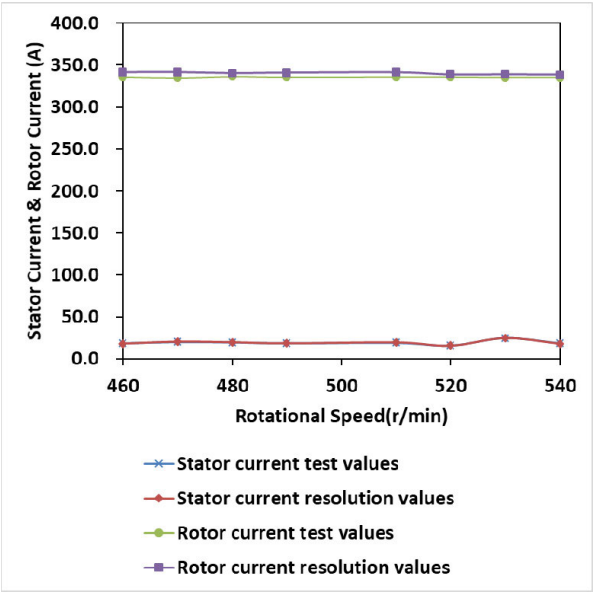

FIGURE 14. Stator and rotor current test and analysis comparison curve in speed control test.

(i) In the speed regulation test, the stator and rotor currents remain unchanged, which is consistent with that described in III.A;

TABLE 4. Comparison of test results for regulated active power.

Binding conditions	Stator current/A			Rotor current/A		
	Test value	Parse value	Err/ %	Test value	Parse value	Err/ %
point 1: ①n=466r/min ②Ps=-4682kW ③Qs=-89kVar	264.1	262.4	-0.7	381.9	379.1	-0.7
point 2: ①n=466r/min ②Ps=-3595kW ③Qs=-48kVar	201.5	199.2	-1.2	368.1	365.6	-0.7
point 3: ①n=466r/min ②Ps=-2880kW ③Qs=8kVar	161.6	161.5	-0.1	361.0	358.4	-0.7
point 4: ①n=466r/min ②Ps=-1754kW ③Qs=-55kVar	98.3	98.5	0.2	353.4	350.1	-0.9
point 5: ①n=466r/min ②Ps=-767kW ③Qs=-129kVar	43.2	43.7	1.0	349.6	346.0	-1.0

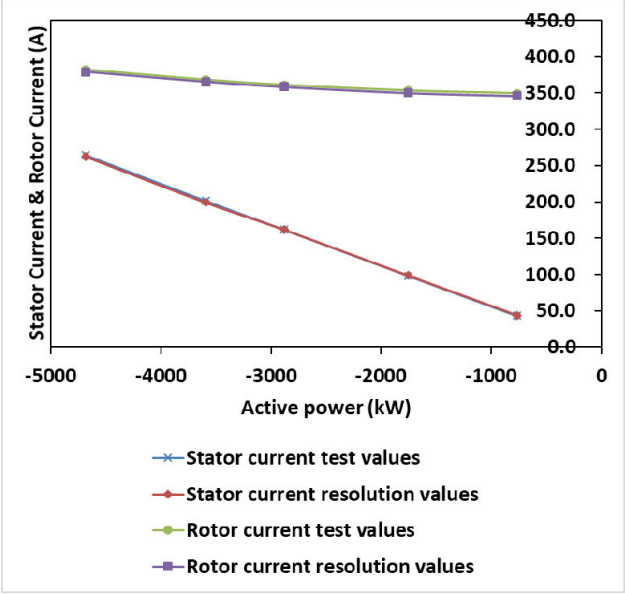

FIGURE 15. Stator and rotor current test and analysis comparison curves in the active power test.

(ii) The calculated values from the analysis of the operating characteristics model established are basically consistent with the test values, verifying the accuracy of the mathematical model;

(iii) The local grid voltage during the test was 10.3 kV, so the rotor current during the test was smaller than the rated no-load excitation current, and there were small fluctuations in the active stator power when the motor was running on the grid, which will not be repeated subsequently.

TABLE 5. Comparison of test results for regulated reactive power.

Binding conditions	Stator current/A			Rotor current/A		
	Test value	Parse value	Err/%	Test value	Parse value	Err/%
point 1: ①n=470r/min ②Ps=-286kW ③Qs=-814kVar	22.9	23.5	2.8	358.1	368.7	2.9
point 2: ①n=470r/min ②Ps=-283kW ③Qs=-168kVar	18.4	18.7	1.2	340.7	347.2	1.9
point 3: ①n=470r/min ②Ps=-226kW ③Qs=489kVar	30.5	31.3	2.5	322.4	325.4	0.9
point 4: ①n=470r/min ②Ps=-235kW ③Qs=795kVar	45.8	46.6	1.7	308.2	315.1	2.2

C. REGULATED ACTIVE TEST ANALYSIS

In accordance with the standard motor regulation active test, the stator side of the motor under test is run on the network, the motor speed is fixed at 466r/min, the active power of the variable speed motor-generator is regulated, the active power, reactive power, stator voltage, stator current and excitation current on the stator side are recorded, the same operating conditions are analysed and calculated using the operating characteristics analysis model, and the comparison results are shown in Table 4. The curves of the stator and rotor currents with the stator active power at the five operating points during the regulated active power test are plotted as shown in Fig.15. As it was not possible to switch directly from power generation to electric operation, the data in the table only shows the results of the power regulation tests in power generation.

An inspection of the data in Table 4 and the comparison curves in Fig.15 shows that:

(i) In the active power regulation test, as the output active power decreases, the stator and rotor currents become smaller, and the stator current changes are larger, in line with what is described in III.B;

(ii) The calculated values are basically the same as the test values using the analysis of the established operating characteristics model, which verifies the accuracy of the mathematical model.

D. REGULATED REACTIVE POWER TEST ANALYSIS

In accordance with the standard motor regulation reactive power test, the stator side of the motor under test is run on the network, the motor speed is fixed at 470 r/min, the reactive power of the variable speed motor-generator is regulated, the active power, reactive power, stator voltage, stator current and excitation current on the stator side are recorded, the same operating conditions are analysed and calculated using the

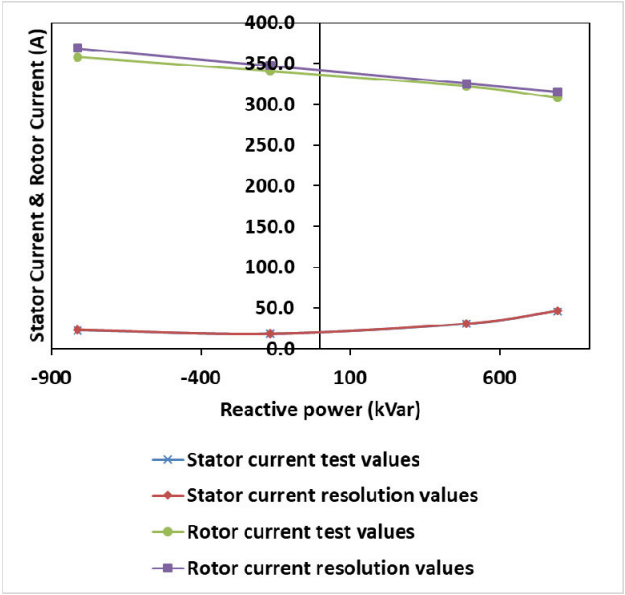

FIGURE 16. Stator and rotor current test and analysis comparison curves in the reactive power test.

operating characteristics analysis model, and the comparison results data are shown in Table 5. The curves of the stator and rotor currents with stator reactive power at the four operating points during the regulated reactive power test are plotted, as shown in Fig.16.

An inspection of the data in Table 5 and the comparison curves in Figure 16 shows that:

(i) In the reactive power regulation test, the stator reactive power decreases and then increases when the stator current decreases from issuing reactive power to absorbing reactive power; the rotor current gradually decreases, which is consistent with that described in III.C;

(ii) The calculated values are basically the same as the test values using the analysis of the established operating characteristics model, which verifies the accuracy of the mathematical model.

V. CONCLUSION

This paper fully considers the demand of variable speed pumped storage motor-generator for multi-state dynamic conversion, combines the characteristics of variable speed motor-generator for bi-directional energy flow, takes into account the complex control strategy caused by its two operating modes of power generator and electric power, and clarifies the constraint law affecting the electrical quantity of motor-generator under different operating conditions, so as to lay the foundation for the stable operation of variable speed motor-generator system. Starting from the analysis of the mathematical model of the two simultaneous rotating coordinates of the variable-speed power motor, the mathematical model of the operation characteristics analysis is derived in detail, and the electrical quantities during the speed regulation, active power regulation and reactive power regulation of the power motor are calculated using the mathematical model, and the change rules of the electrical quantities such as stator and rotor currents, rotor voltage, rotor active power, rotor reactive power and stator power angle are summarized during the change of operating conditions. Finally, a no-load test, a speed test, a regulated active test and a regulated reactive test were carried out on the 10MW prototype. By analysing the variation patterns of the stator and rotor currents in the test results and comparing the test results with the analytical calculation results, the correctness of using the mathematical model of operating characteristic analysis to generalise the variation patterns of electrical quantities was verified on the one hand, and the accuracy of the analytical calculation results of the mathematical model of operating characteristic analysis was verified on the other. On the other hand, the accuracy of the analytical calculation results of the mathematical model of operating characteristics analysis is verified. The 10MW test prototype developed in this paper is the largest variable speed test prototype in China at present, and the joint test with the converter has been completed. The test results lay the foundation for the Chinese construction of large variable speed pumped storage power plants.

REFERENCES

[1] M. Han, X. Chang, J. Li, G. Yang, and T. Shang, "The application and development of pumped storage technology," *Sci. Technol. Herald*, vol. 34, no. 23, pp. 57–67, Dec. 2016.

[2] G. Zhang, Y. Chen, J. Zhang, N. Tang, and Y. Niu, "Day-ahead optimal scheduling of wind-light-water-fire-pumped storage co-generation system," *J. Sol. Energy*, vol. 41, no. 8, pp. 79–85, Aug. 2020.

[3] X. Zhang, P. Zhang, and X. Chen, "Development and application of seawater pumped storage power plants," *Hydropower Station Electromech. Technol.*, vol. 42, no. 6, pp. 66–70, Jun. 2019.

[4] J. Zhao and T. Wang, "Analysis of the necessity of applying variable speed units in Fengning II pumped storage power plant," *China High-Tech Enterprise*, vol. 7, pp. 118–119, Feb. 2016.

[5] W. Cai, Y. Wang, H. Shi, M. Zhang, and Q. Xu, "Study of speed and opening optimization strategy for large variable speed pumped storage units," *Large Electr. Mach. Technol.*, vol. 4, pp. 58–63, Jul. 2020.

[6] T. Zhang, H. Wang, and D. Qin, "Analysis of pump selection characteristics of variable speed water pump turbine," *Large Electr. Mach. Technol.*, vol. 2, pp. 65–69, Mar. 2020.

[7] C. Zhang, Y. Sun, F. Wang, and H. Zhang, "Analysis of electromagnetic performance of variable speed pumped storage power motors," *Large Electr. Mach. Technol.*, vol. 5, pp. 6–10, Sep. 2020.

[8] Z. Wei, S. Huang, X. Tao, and C. Gu, "Operating principle and steady-state performance analysis of a variable-speed, constant-frequency doubly-fed generator," *J. Huazhong Univ. Technol.*, vol. 5, pp. 34–37, May 1996.

[9] Y. Zhu, "1.25MW doubly-fed asynchronous wind turbine design," *J. Shanghai Inst. Electr. Eng.*, vol. 12, no. 1, pp. 84–86, Mar. 2009.

[10] F. Wang, H. Lv, Y. Zhao, H. Wang, J. Wang, W. Zhou, and W. Wang, "Research and design of 6.5 MW variable speed hydro generator set," *J. Eng., Heilongjiang Univ.*, vol. 5, no. 1, pp. 78–83, Mar. 2014.

[11] A. Joseph, K. Desingu, R. R. Semwal, T. R. Chelliah, and D. Khare, "Dynamic performance of pumping mode of 250 MW variable speed hydro-generating unit subjected to power and control circuit faults," *IEEE Trans. Energy Convers.*, vol. 33, no. 1, pp. 430–441, Mar. 2018.

[12] W. Hu, H. Fan, and Z. Wang, "Simulation and control of power regulation of doubly-fed pumped storage units," *J. Tsinghua Univ. Natural Sci. Ed.*, vol. 61, no. 6, pp. 591–600, Jul. 2021.

[13] H. Sun, S. Fang, S. Xu, J. Bi, J. Yi, R. Song, and L. Gao, "Small disturbance stability analysis and control of wind power grid-connected systems based on Nyquist array theory," *Chin. J. Electr. Eng.*, vol. 40, no. 10, pp. 3124–3134, Apr. 2020.

[14] X. Yan, S. Cui, X. Sun, Y. Sun, Z. Song, W. Liu, B. Cao, and T. Li, "Modeling of double-fed wind turbines for full operation and fast start-up electromagnetic transients," *Power Grid Technol.*, vol. 45, no. 4, pp. 1250–1260, Apr. 2021.
[15] X. Wang, M. Han, and G. Bitew, "Analysis of reactive power characteristics of doubly-fed variable speed pumped storage units," *Power Grid Technol.*, vol. 43, no. 8, pp. 2918–2925, Apr. 2019.
[16] J. You, W. Ning, H. Jiang, Y. Dong, H. Liu, and Y. Li, "Impedance characteristics of DFIGs considering the impacts of DFIG numbers and its application on SSR analysis," *IOP Conf. Ser., Mater. Sci. Eng.*, vol. 199, pp. 215–223, May 2017.
[17] X. Hua, X. Hongyuan, and L. Na, "Control strategy of DFIG wind turbine in primary frequency regulation," in *Proc. 13th IEEE Conf. Ind. Electron. Appl. (ICIEA)*, May 2018, pp. 1751–1755.
[18] A. Djoudi, E. Berkouk, S. Bacha, and H. Chekireb, "Real time estimation of DFIG inductances and rotor currents," in *Proc. 3rd Renew. Power Gener. Conf. (RPG)*, 2014, pp. 1–5.
[19] C. Wu, B. Hu, P. Cheng, H. Nian, and F. Blaabjerg, "Eliminating frequency coupling of DFIG system using a complex vector PLL," in *Proc. IEEE Appl. Power Electron. Conf. Expo. (APEC)*, Mar. 2020, pp. 3262–3266.
[20] G. Mu, T. Cai, G. Yan, H. Liu, and S. Liu, "Bidirectional power constraint of doubly-fed wind turbines participating in continuous frequency regulation and its effects," *J. Electr. Eng. Technol.*, vol. 34, no. 8, pp. 1750–1759, Mar. 2019.
[21] X. Yu, Y. Zhu, and C. Gao, "Study of control strategy for fast power response of doubly-fed hydro generator," *J. Hydropower Gener.*, vol. 38, no. 5, pp. 89–96, Jan. 2019.

HU JINMING was born in 1992. He received the B.S. degree in electrical engineering and automation from the China University of Mining and Technology, Beijing, in 2015, and the M.S. degree in electrical engineering from the Harbin University of Science and Technology, Harbin, China, in 2021. Currently, he is with Harbin Electric Machinery Company Ltd., engaged in large generator design and motor dynamic performance analysis.

TAO DAJUN was born in Xiangyang, China, in 1982. He received the B.S., M.S., and Ph.D. degrees in electrical machinery and appliances from the Harbin University of Science and Technology, Harbin, China, in 2005, 2008, and 2013, respectively. He is currently an Associate Professor with the Harbin University of Science and Technology. His research interests include basic theory and application technology of large electric machine, theory, design, and analysis of novel special motor.

SUN YUTIAN was born in 1963. He received the Ph.D. degree in electrical machines and apparatus from the Shenyang University of Technology, Shenyang, China, in 1998. Currently, he is with the Harbin Research Institute of Large Electrical Machinery, engaged in the development of hydro-generators, motor-generators, turbo-generators, and large motors.

ZHANG CHUNLI was born in 1975. She received the B.S. and M.S. degrees in electrical engineering from the Harbin Institute of Technology, China, in 1997 and 2007, respectively. Currently, she is with Harbin Electric Machinery Company Ltd., engaged in FM analysis and the design of machines.

LI GUIFEN was born in 1978. She received the B.S. and M.S. degrees in electrical engineering from the Harbin University of Science and Technology, Harbin, China, in 2000 and 2014, respectively. Currently, she is with Harbin Electric Machinery Company Ltd., engaged in large generator electromagnetic design and dynamic performance analysis.

HU GANG was born in 1982. He is a Senior Engineer with Harbin Electric Machinery Company Ltd. He has been engaged in the research and simulation of electromagnetic theory for large generator, since 2008. He has participated in the research and development of many significant projects, such as Baihetan 1000MW Hydro-Generator and Yangjiang 400MW Generator-Motor.